Int J Adv Manuf Technol (2012) 59:377–395
DOI 10.1007/s00170-011-3501-5

ORIGINAL ARTICLE

Contact states recognition in robotic part mating based on support vector machines

Zivana Jakovljevic · Petar B. Petrovic · Janko Hodolic

Received: 1 March 2011 / Accepted: 26 June 2011 / Published online: 10 July 2011

Abstract In order to autonomously execute part mating, an intelligent robot should be able to carry out active compliant motion. Contact states recognition machine is a missing link for implementation of this kind of motion within an intelligent robotic assembly system. In this paper, we present an approach to design contact states recognition machines for various types of part mating problems. We have chosen generalized mating force as a basic feature measured from the process. Starting from force measurements, online recognition is carried out using class boundaries and transduction mappings obtained during offline training. The basis for the proposed offline training procedure is not experimental data but a mechanical model of the part mating process. This enables supervised training without requiring numerous experiments. Furthermore, this has allowed extraction of qualitative features from the analytical model of mating force. To provide good time localization and phase correctness, we have utilized discrete wavelet transform for feature extraction. The obtained patterns have been classified using support vector machines to obtain a recognition machine with good generalization properties. The proposed machine is elaborated and experimentally verified using case study of cylindrical part mating with chamfer crossing. We have used quasi-static model of insertion force as a starting point in the training process. Exploiting some characteristics of Daubechies wavelets, we have managed to extract features that are independent on characteristics of the concrete cylindrical part mating. Finally, the generated machine was evaluated using intensive real-world experiments. Herein we have shown that performance of the generated contact states recognition machine was excellent.

Keywords Support vector machines · Part mating · Discrete wavelet transform

Abbreviations

NN	Neural network
HMM	Hidden Markov model
MO	Moving object
EO	Environmental object
CS	Contact state
PC	Principal contact
DWT	Discrete wavelet transform
SVM	Support vector machines
WT	Wavelet transform
CWT	Continuous wavelet transform
MRA	Multiresolution analysis

1 Introduction

Part mating process is one of the basic assembly operations. It represents the mating of a moving object (moved by human, robot, or some other device) and an environmental object. During the robotic part mating, gross and fine motions can be identified. Gross motions are used to move parts over distances which are very large with respect to the parts' size. During these motions, the parts are not in contact, and therefore, there is no need for high accuracy.

Z. Jakovljevic (✉) · P. B. Petrovic
Faculty of Mechanical Engineering, University of Belgrade,
Kraljice Marije 16,
11000 Belgrade, Serbia
e-mail: zjakovljevic@mas.bg.ac.rs

J. Hodolic
Faculty of Technical Sciences, University of Novi Sad,
Trg Dositeja Obradovica 6,
21000 Novi Sad, Serbia

On the other hand, fine motions represent the part mating itself. During the fine motions, parts are generally in contact and small errors (of the clearance size) can cause very large interaction forces. This can lead to disturbances or even failure of the part mating process as a whole. Although the errors are usually too small for visual detection, they can be haptically sensed. During gross motions, an intelligent robot is able to make changes in programmed position/orientation using artificial vision systems. However, vision-based systems cannot be used to control fine motions for parts with small clearances, since even a small position error can block the part mating process. Therefore, in these cases, a control which utilizes the force feedback has to be employed.

During part mating, significant uncertainties are inherently present in robot environment. These uncertainties lead to errors during fine motions. Their origin can be geometrical (e.g., parts tolerances, position of environmental object, position of robot gripper, sliding of moving object in gripper) and dynamical (e.g., rigidity of the system, elasticity of parts in contact, uncertainties in the friction model). The most effective solution for part mating in such environment is active compliant robot motion.

Instead of following a predefined geometrical trajectory, with the active compliance control, the robot starts to simultaneously follow the force trajectory previously defined by the force control law. Therefore, with this control scheme, the robot can optimally perform various tasks without any hardware changes. Active compliant motion is an indispensable component of an intelligent assembly robot as long as the intelligence incorporates ability to reliably, flexibly, and effectively accomplish the desired interactions between the robot and its environment full of uncertainties [1]. Although the number of robotic applications in industrial assembly tasks is increasing over the years, the application of intelligent robotic assembly systems is still in its infancy [2]. One of the missing elements is the active compliant robot motion.

Part mating is a highly nonlinear dynamical process. A lot of research activities were carried out in the field of modeling and control of nonlinear systems [3–7]. The neural networks, fuzzy logic, genetic algorithms, etc. have been extensively employed. Nevertheless, the proposed methods cannot be straightforwardly used due to a number of reasons. Primarily, the analytical model of the mating system has no unique structure. The general model is comprised of a set of analytical equations, where each equation describes a particular contact state. For the given case of part mating process, the contact states are arbitrarily changing. Therefore, the obtained overall analytical model is variable and discontinuous. The specificity of the part mating system is that its analytical model has a variable structure which is unknown in advance. Its structure can be determined only after the whole set of contact states, and their transitions have been recognized. In the real time, only partial models are relevant, depending on the current contact state. Therefore, the recognition of the contact states is essential for successful part mating process based on the active compliant motion.

There are two approaches in previous work in the area of the contact state recognition. One group of researchers starts from analytical model of the part mating process, and using statistical methods determines the similarity between the actual and modeled situation [8–19]. The level of similarity is used to determine the current contact state. The other approach utilizes a large collection of experimental data to learn contact states using different soft computing techniques (e.g., neural networks (NNs), fuzzy logic, Hidden Markov models (HMMs)) [20–36].

Early methods [8–10], which start from analytical models, were based on separating (polyhedral convex) cones derived from geometrical and quasi-static models of contacting parts. It was assumed that the separating cone contains the directions of all the forces that could act on parts during the given contact state. Nevertheless, the authors themselves [8] concluded that due to significant uncertainties, it was not always possible to differentiate all contact states using the proposed methodology. Another approach [11–14] was based on finding all possible contacts by building polyhedral objects using the estimated uncertainty of contacts' location. Recent work considered the estimation of geometrical parameters using Kalman filters [15–18]. The geometric parameters were estimated assuming that the contact state was always compliant with the motion plan. The transition between contact states could be recognized using the inconsistency of measured values and the current model [18]. The extension of this work has been presented in [19] where the transition particle filters have been proposed for recognition of the contact states. The main limitation of this method is that contact states could be recognized only after they were well established—only after the dynamic region at contact transition has passed. Therefore, this method introduces a very large latency since the time needed for the recognition was high.

The aforementioned methods, based on analytical models, mainly address the part mating problems in which both parts can be described as convex polyhedra and contact states are made of a single principal contact. Nevertheless, when one of the parts is concave, the contact state can have more than one principal contact. In these situations, the previous work implied learning of contact states based on considerable amount of experimental data. As the research in the field of contact states recognition moves forward, it becomes clear that, as a result of nonlinearity and a truly dynamical nature of the problem, the learning process must incorporate sophisticated techniques (e.g., methods that

apply NNs, their combination with fuzzy logic, advanced statistics).

NNs and reinforcement learning technique were applied in learning of cylindrical part mating task in [20]. In [21], the authors proposed a method that can be used to learn the process of placing the cube on the plane. They introduced two classifiers—one based on fuzzy logic and the other based on NNs—and showed that the classifier based on fuzzy logic outperformed the NN classifier. In this work, the features used for classification were normalized values of the mating force. However, the proposed methods require extensive training, and with the change of the contact position relative to the sensor (e.g., the change in object's dimension), the training should be carried out again. In [22], the same authors proposed a method for classification performance retrieval in such a case, but the results were very limited with respect to the change in parts' dimensions.

Correlation of the measured force and pose (position and orientation) with actions carried out during peg-in-hole part mating was learned applying reinforcement learning in [23]. The features used for the learning were discretized values of the measured force and pose components. The authors considered insertion of different parts (circular, quadrangular, and triangular prisms). In [24], the contact states in peg-in-hole part mating were learned using NN where the features were normalized decoupled force components.

Fuzzy set theory and NNs for contact states recognition were integrated in [25], where the normalized values of force components were used as features. Another approach that assumed the combination of fuzzy logic and NNs is proposed in [26, 27]. In these works, the author focuses on a selection of a motion plan (among all possible motion plans) that would lead to successful insertion without wedging. Uniformly discretized features obtained from the wedging diagram [28] were chosen as a learning basis.

Structure of HMMs makes them suitable to recognition of processes that imply state transition. Therefore, the use of HMMs for contact states recognition has obtained considerable attention. The first application of HMMs in the compliant motion was in the modeling of the forces that human operators apply during cylindrical part mating in telemanipulation task [29]. Research work presented in [30] gives the methodology for recognition of contact states transition using HMMs. For each transition, a HMM was created. Observation symbols (input features) were the spectral components of generalized force signals. Similar approach is given in [31], where the observation symbols were the values of the generalized mating force which was processed using vector quantization technique. Different from other approaches which were based on force measurements, in [32] the authors proposed contact states recognition using pose measurements. The observation symbol was the difference between theoretically computed value of the contact pose in environmental frame and the measured pose in the robot gripper frame. HMMs were created for each contact state.

Template matching for recognition of contact states was proposed in [33]. Although the authors emphasize the need for qualitative features, the features they used were based on quantitative thresholding of the force signal. An extension of this work from [34] proposed a machine for recognition of contact states transitions using the distance clustering technique and finite state machines.

The method for recognition of contact states for automated height adjustment of a cylindrical lower pair is given in [35]. The estimated level of contact force components and the parameter called d_{value} were used as features. Here, d_{value} was extracted from the model of contact forces, and it was highly dependent on the friction coefficient. The proposed approach assumed that the two point contact is possible only after the outer link has completely (with both edges) passed the rim of the inner link. However, this assumption is not always justified, especially in scenarios where the clearance between mating parts is small. Besides, two essentially different single point contacts in the cylindrical part mating could not be differed using the proposed methodology.

In [36], the force–torque maps were proposed for estimation of the pose error, where the generated maps had redundant areas. It was proposed that the tilting angle between mating parts should be changed to move from redundant areas. Using this approach, a large number of attempts had to be performed before the parts were mated, which made this method very impractical and time-consuming.

Based on the presented analysis, we can note that the methods which start from analytical models did not offer reliable and real-time applicable methodology for contact states recognition. The methods that implied learning of contact states were based on extensive experiments. Some of them considered the cube on plane [21, 22, 31] and the others considered various forms of peg-in-hole part mating [23, 30, 33, 35, 36]. Peg-in-hole experiments were conducted using materials not frequently utilized in practice (e.g., plastics [33], wood [23]), or with parts with huge clearances [23, 30, 35, 36]. For example, the clearance in [35] was 1 mm with nominal diameter of 30 mm, and in [36], it was 0.95 mm with nominal diameter of 97 mm.

When the machine for contact states recognition is created strictly based on experimental data, the following problems arise: (1) it is not possible to infer which contact state is present at each instant during the experiments and (2) a large number of experiments with uncertain outcomes have to be performed (as the generated forces can be high due to the large uncertainties and small clearances in the

process). The qualitative features can hardly be extracted since the only available information is the mating force vector. Since the features are quantitative, created machines can be applied only in the processes whose parameters (e.g., part materials, dimensions, relative clearances, rigidity) are very similar to those used in the experiments. Therefore, the designed machine cannot be generally applicable.

The aforementioned learning techniques have been based on experimental data. The features used for learning in these techniques have been quantitative and based on the rigid thresholding and uniform discretization of the mating force.

In this paper, we address the problem of precise part mating which is a common task in mechanical engineering. A typical example is the bearing insertion where the clearance is of the micrometer size, and the hardness of contact surfaces is very high (50–60 HRC and even more). The small clearance and high hardness of mating surfaces essentially change the nature of the part mating task. In these scenarios, the clearance is far below the resolution and accuracy of the robot control system, which is typically in the range of 0.02 up to 0.2 mm. Under these circumstances, the effects of uncertainties become very important, and the features used for learning have to be qualitative.

We propose a new general framework for synthesis of information machines used for contact state recognition. Opposite to the existing techniques, we start from the mechanical model of the mating force. This allows us to extract truly qualitative features. These features are independent of the force level and the parameters of the current part mating process [37]. In this way, we obtain general applicability for the modeled class of tasks (e.g., cylindrical peg-in-hole, or cube-into-corner).

We employ discrete wavelet transform (DWT) as a formal tool for generation of qualitative features from the acquired force signal. Furthermore, we exploit the analytical properties of the wavelets instead of choosing them arbitrarily (which is a common practice). Since we work with a dynamical nonlinear process, the model used for feature extraction is approximate. Therefore, to deal with modeling error and to introduce additional robustness to the real-world recognition system, we use support vector machines (SVM), which classify the contact using the extracted feature vectors.

The rest of the paper is organized as follows: We first give the task setting in Section 2. Then, in Section 3, the general framework for creation of machines for contact states recognition is proposed. In Section 4, we elaborate the proposed architecture using cylindrical peg-in-hole part mating as an example. We describe how the truly qualitative features can be extracted from the force model and how the robust class boundaries can be generated. Section 5 gives the results of experimental verification, which illustrate the real-world applicability of the proposed methodology. Finally, we give concluding remarks and an avenue for future work.

2 Task setting

During part mating, the robot is in interaction with the environment that constrains its motion. To perform this kind of task, the robot should comply with the interaction forces. It should perform a compliant motion which assumes the correction of the nominal trajectory depending on interaction forces. Active compliant motion is realized using force feedback. It starts from the assumption that each contact situation between the moving object (MO) and the environmental object (EO) generates a specific response in the form of generalized force (force/torque.)

The parts in contact are 3D objects contacting trough surface elements (i.e., faces, edges, and vertices). In order to describe different contact formations between mating objects, Desai and Volz introduce elemental contacts in [8]. Due to significant uncertainties in the part mating process, it was impossible to distinguish contact formations based on the elemental contacts, so the principal contacts have been introduced in [11].

To define contact state, we introduce the following formal definitions:

> **Definition 1:** *Contact feature* (CF) is a surface element of an object in contact that is not the boundary element of another surface element in the same contact. Contact feature CF = $\{f, e, v\}$, where f is a face, e is an edge that is not the boundary edge of a surface in the same contact, and v is a vertex that is not the boundary vertex of an edge or a face in the same contact.
>
> **Definition 2** [11]: *Principal contact* (*PC*) is the unique pair of contact features PC = (CF^i_A, CF^j_B), where CF^i_A and CF^j_B are contacting features i and j of mating parts A and B.
>
> **Definition 3**: *Contact state* (CS) is a set of principal contacts CS = $\{PC_i, PC_j, \ldots PC_k\}$.

When both mating parts are convex, all CSs between them consist of only one PC. When one of the mating parts is concave, there are CSs that consist of more than one PC. The recognition of CS in the latter case is more complex. Generally, with each PC, additional degrees of freedom are taken from the system, and the control task becomes more complex.

For illustration, some of the principal contacts and contact states between trihedron and tetrahedron are shown in Fig. 1. A large number of contact states can be differentiated for such simple parts. For more complex parts, the number of possible contact states is even larger.

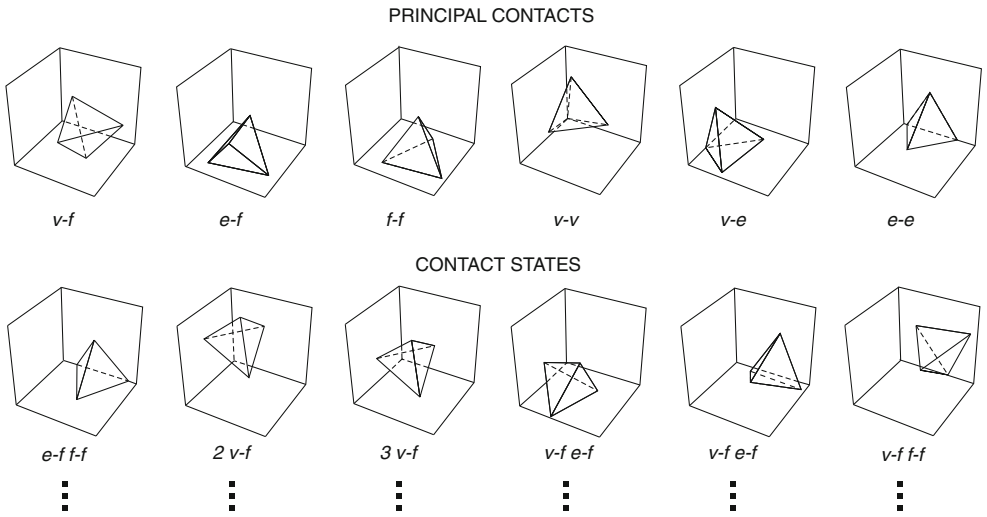

Fig. 1 Some of the principal contacts and contact states between trihedron and tetrahedron; *f* face, *e* edge, *v* vertex

The architecture of the system for active compliant robot motion is presented in Fig. 2. It has the following active components: (1) interactive planner which is able to re-plan in real time, (2) system for recognition of contacts, and (3) controller for execution of compliant motion commands.

Beside the aforementioned active components, an active system for compliant robot motion incorporates a model of the process. This model includes a geometrical and topological representation of the objects, the set of their contact states, and possible transitions between these states. Furthermore, it includes a mechanical model that provides information about forces that can be generated during a compliant motion.

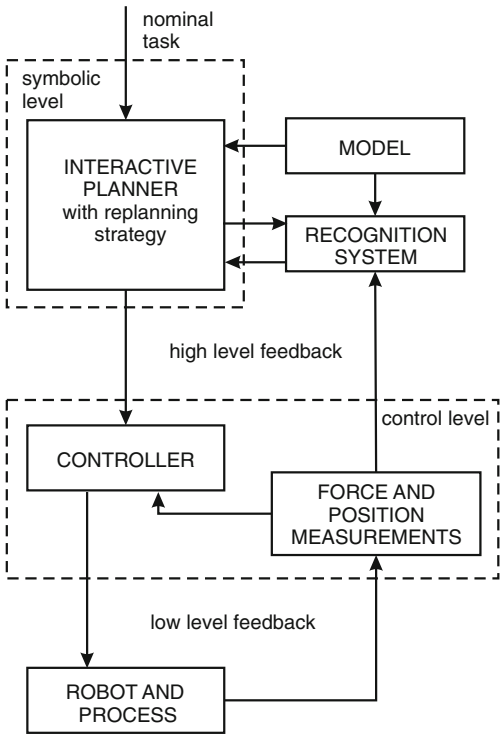

Fig. 2 The architecture of the system for active compliant robot motion

In an active system for compliant motion (Fig. 2), the controller gets a set of points from the planner, compares it with measurements from the robot system, and calculates corresponding commands for joints actuators. It is responsible for turning the plan into real robot's actions in its environment.

The interactive planner (Fig. 2) working at the symbolic level creates plans for active motion commands. Its role is to synthesize the robot's trajectory based on collision constraints that are present in the process. The constraints are not known in advance since an active compliant motion system operates in a semi-structured or unstructured environment full of uncertainties. It is necessary for a planner to be able to re-plan the trajectory based on data obtained from the process in real-time.

To provide this high level feedback, we introduce a system for contact recognition (Fig. 2). Its role is to recognize the contact states and to estimate geometrical parameters and dynamical properties of the environment. The recognition system transforms the sensory information (i.e., force and/or pose) into the corresponding symbols which can be used as planner input. It is the interface between the planner controlling the mating process at high symbolic level and the controller which is used to for the low level feedback control. The recognition system can make estimation of geometrical and dynamical parameters only if the contact state is correctly identified. The recognition system gives the perception capability to the robot. It enables its environmental awareness and provides certain elements of intelligence to the active system for compliant motion.

A vast amount of research has focused on different components required for active compliant motion system. However, there is a lack of research that is focused on the interfaces between these components [38]. The missing

links are (1) transformation of planner outputs into the low level specifications compatible with the controller and (2) the upgrade of the recognition system with functions that transform the low level measurement signals into the high level contact primitives (i.e., contact states) used by the planner. The latter especially requires additional work since it is the crucial link needed to provide a valuable feedback to the planner.

3 Architecture of contact state recognition machine

In this section, we present the machine for recognition of contact states. The machine has two modules: one is used for offline training, and the other is utilized for online recognition.

Part mating is dominantly a geometrical problem. Thus, if the parts were perfectly positioned, the problem would be very easy to solve. Nevertheless, due to significant uncertainties that are present in the process, this condition is rarely satisfied. In general, the exact relative position of MO and EO is unknown, and the recognition of CS is not easily feasible.

Part mating is a dynamical process in which parts' trajectories and mating forces are correlated. It is not possible to get reliable information about the exact position of the mating objects from the process in real time. However, the mating forces can be easily measured. Therefore, in the proposed CS recognition machine, we have chosen a six-component vector of the generalized mating force **F** acting between MO and EO as the basic feature obtained directly from the process.

The architecture of the proposed machine for online recognition of contact states is presented in Fig. 3. Using transformations $\mathfrak{I}$ (Fig. 3), components of the measured force **F** are transduced into patterns—feature vectors **x**. After the transduction, the classification is carried out to obtain the pattern's class (Fig. 3) that corresponds to the contact state currently present in the process. Information about the current contact state is handed over to the planner, thus providing a valuable real-time feedback at the symbolic level. The planner, based on the motion plan and the current contact state, gives commands to the robot control system for further actions (i.e., trajectory correction). Transformations $\mathfrak{I}$ used in transduction as well as class boundaries utilized in classification are defined during the offline training process.

The architecture of the proposed offline training is shown in Fig. 4. The main characteristic of the training machine is that it does not start from experimental data, but from the mechanical model of the part mating process at hand. This allows the extraction of qualitative features which was not possible with the previously used methods.

The process model contains its geometrical, topological, and mechanical representation. The geometrical model is defined by geometry of the mating parts, manipulation mechanism elements, environment, fixtures, and other objects in the process. Contact states that can appear during the process are derived from the topological representation.

In order to create a mechanical model, it is necessary to have a geometric representation and a set of all contact states. A mechanical model provides the variations in time of the generalized mating force components along with the accompanying contact states. Different motion equations are valid for different contact states.

Since part mating is a dynamical process, creation of a dynamical model seems reasonable. Nevertheless, part mating is dominantly a geometrical problem and certain approximations to dynamical model should be introduced. Besides, working in real time requires a reasonable model complexity. Therefore, we have opted to utilize a quasi-static model of mating forces.

Starting from a mechanical model, the offline training machine has the information about contact states. It is worth noting here that this information is not available when experimental data are exclusively used. In our approach, it is possible to carry out supervised training. From the modeled mating force vector (**F**), we extract and select the feature vectors (**x**) that are relevant for the following classification.

Feature selection and extraction are the most important parts of every pattern recognition [39]. If the features are representative and discriminative, the classification is trivial and leads to good performance of the pattern recognition as a whole. Finally, after extraction of features, the feature space is partitioned using supervised classification into CS and class boundaries are generated. For the reasons that will be explained in the sequel, we propose DWT for feature extraction and SVM for classification.

3.1 Feature extraction

Transformations $\mathfrak{I}$ come as a result of feature extraction and selection. They can represent physical values measurements but also can contain some signal processing for extraction of more effective features. Part mating is a dynamical, nonlinear, nonstationary process. Contact state transitions are mapped into abrupt changes in measured force signals. Since the objective is to recognize a new contact state as soon as it appears, it is very important that utilized feature extraction techniques have good time localization capabilities. Besides, these techniques should be suitable for real-time applications. For the aforementioned reasons, we use DWT for extraction of features from generalized force measurements.

Wavelet transform (WT) represents signal as a linear superposition of elementary building blocks—atomic func-

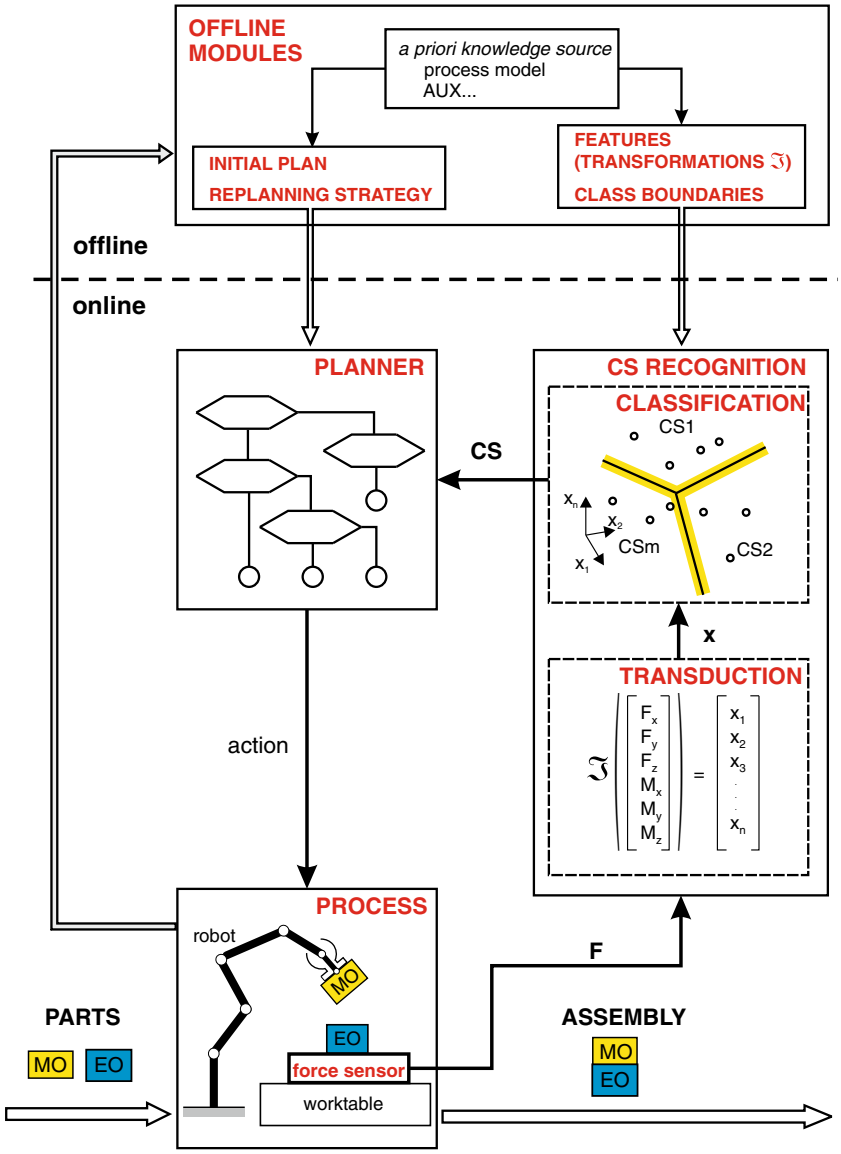

Fig. 3 The architecture of the machine for online contact states recognition

tions [40]. These functions are obtained from a specific function called mother wavelet by dilatation and translation along the time axis. Unlike harmonic functions used in traditionally applied Fourier transform, mother wavelets can have different shapes. They can be compactly supported, thus leading to good time localization of the signal. In addition, they can have asymmetric shapes which make them suitable for analysis of signals with abrupt

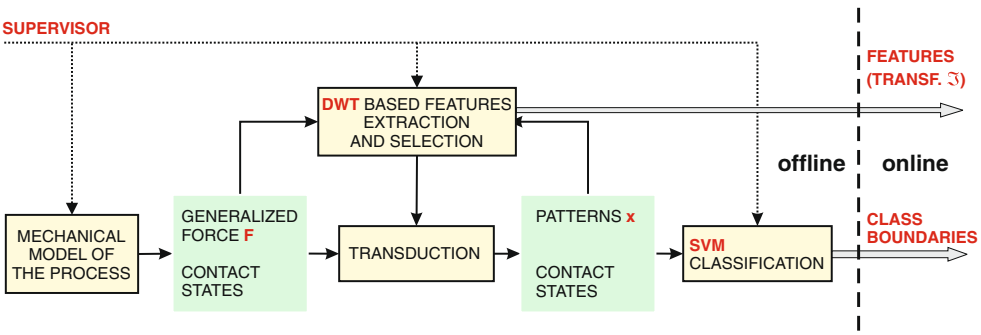

Fig. 4 The architecture of off-line training of the recognition machine

changes. Generally, the only restriction posed to wavelets is that their integral must equal to zero, that is, they must "wave" around time axis.

There are two kinds of WT, continuous (continuous wavelet transform, CWT) and discrete (DWT). In CWT, the mother wavelet is continuously translated along the time axis and dilated gradually from the minimal to the maximal value. In DWT, dilatation is always carried out with a predefined factor, and translation is performed using a discrete step dependent on the dilatation factor. CWT has better resolution but the algorithms for its implementation require more processing time compared to algorithms used for DWT. Thus, DWT is more suitable for real-time applications.

The wavelets used for DWT must fulfill additional conditions (besides "waving" around time axis). They must form an orthonormal basis [40]. DWT can be represented as given in Eq. 1:

$$T_{m,n} = \int f(t) a_0^{-m/2} \overline{\psi(a_0^{-m/2} t - n b_0)} \mathrm{d}t \tag{1}$$

where $f(t)$ denotes the analyzed signal, ψ is the mother wavelet, ${a_0}^m$, $m \in \mathbf{Z}$ is the discretization of dilatation parameter (a_0 is the dilation step such that $a_0 \neq 1$), and b_0 denotes the translation step, while over-line stands for complex conjugate. Given discretization insures that narrow wavelets containing high-frequency components are translated in small time steps, while wide wavelets containing low frequencies are translated in larger time steps. Therefore, DWT has better time resolution for high and better frequency resolution for low frequencies.

Multiresolution analysis (MRA) [41], emerged from research performed in image processing, gives a suitable way to create orthonormal wavelet bases as well as fast algorithms for implementation of direct and inverse DWT. Without getting into the details of MRA derivations, its basic results are presented here. For more details, refer to [41].

For the sequence of resolutions 2^j, $j \in (0, -\infty)$, each signal f can be represented as a sum of its approximation $A_J f$ at a given level (i.e., resolution) J and details $D_j f$, $j \in [0, J]$ taken from it while passing from one level of approximation to the next one. This can be formulated as:

$$f = A_J f + \sum_{j=1}^{J} D_j f = \sum_n a_n^J \phi_{J,n} + \sum_{j=1}^{J} \sum_n d_n^j \psi_{j,n} \tag{2}$$

Signal's approximations and details are described using approximation (${a_n}^J$) and detail (${d_n}^j$) coefficients that represent the share of the corresponding scaling functions $\phi_{J,n}$ and wavelets $\psi_{j,n}$ in the signal. It should be noted that, in order to make DWT signal representation unique, it is necessary that the families of functions $\{\psi_{j,n}, j,n \in \mathbf{Z}\}$ and $\{\phi_{J,n}, j,n \in \mathbf{Z}\}$ make orthonormal bases.

Coefficients ${a_n}^j$ and ${d_n}^j$ are computed by so-called subband filtering scheme [41], formulated as:

$$d_k^j = \sum_n \overline{g_{n-2k}} a_n^{j-1} \tag{3}$$

$$a_k^j = \sum_n \overline{h_{n-2k}} a_n^{j-1} \tag{4}$$

The above relations represent convolutions of sequence ${a_n}^{j-1}$, $n \in \mathbf{Z}$ with filters $\overline{H}$ and $\overline{G}$, followed by downsampling by two. Impulse responses of filters $\overline{H}$ and $\overline{G}$ are given by (h_{-n}), $n \in \mathbf{Z}$ and (g_{-n}), $n \in \mathbf{Z}$.

A large number of wavelets that form an orthonormal basis and that can be employed for DWT have been created [40]. The choice of a wavelet used for extraction of features utilizing DWT depends on wavelet characteristics and desired results. Characteristics of a number of wavelet families useful for extraction of different contents from signals can be found in [40].

The wavelet transform has been extensively applied for feature extraction in various engineering tasks [42–45]. Nevertheless, in these studies, the type of wavelet was arbitrarily/intuitively selected without any explanation. In our study, we adopt a different approach. Instead of choosing wavelet arbitrarily or by trial and error, we exploit mathematically formalized properties of certain wavelets for their selection. In Section 4, we show how the wavelet can be selected based on its analytical properties.

3.2 Class boundaries generation

Classification into contact states follows transduction, during the offline training (Fig. 4). Since we start from a mechanical model rather than from experimental data, we can correlate each pattern with corresponding contact state. Therefore, we have been able to obtain supervised learning of classification machine.

The classification needs to be performed in an unstructured environment full of uncertainties. Thus, a suitable classification technique has to be applicable in real time with good generalization properties. These are the main reasons for the use of SVM for classification.

Support vector machines consider learning problem as a problem of minimization of the actual risk [46]. The actual risk is bounded by the sum of empirical risk and confidence interval. With the increase of recognition machine complexity empirical risk is reduced, but the confidence interval

is increased. The minimization of empirical risk does not necessarily lead to minimization of the actual risk. Unlike other recognition machines (e.g., neural networks[1]), SVM start from structural risk minimization which simultaneously minimizes empirical risk and confidence interval. Empirical risk is kept fixed (e.g., equal to zero) and the confidence interval is minimized. Using these machines, minimum of empirical risk simultaneously leads to minimum of actual risk. Consequently, obtained recognition machines have good generalization properties. Generalization property of a recognition machine represents its ability to properly decide about unknown data, based on the knowledge obtained from the training set. Since part mating process is full of uncertainties, excellent generalization properties of SVM are essential for their use in the contact state recognition machine.

SVM start from a training data set $\{(\mathbf{x_1}, y_1), (\boldsymbol{x_2}, y_2) \ldots (\mathbf{x_l}, y_l)\}$ where $\mathbf{x_i}$ denotes the patterns and $y_i \in \{\pm 1\}$ denotes the decision variables that specify the membership of each pattern to one of the classes. For the case of linearly separable data, it is possible to linearly separate the given training set in infinitely many ways using hyperplanes:

$$y_i[(\mathbf{w} \cdot \mathbf{x_i}) - b] \geq 1, i = 1, 2, \ldots l \tag{5}$$

SVM determine the optimal hyperplane from the set of all possible hyperplanes. This hyperplane separates the data without error and provides maximal margin $\Delta = 1/|\mathbf{w}|$ between the hyperplane and the closest pattern in the training set.

For linearly nonseparable data, positive slack variables ξ_i are introduced in decision boundary (Eq. 5). In the case of classification error, $\xi_i \geq 1$. The violation of separating condition 5 is expressed in the following way:

$$y_i[(\mathbf{w} \cdot \mathbf{x}) - b] \geq 1 - \xi_i, i = 1, 2, \ldots l \tag{6}$$

In order to determine the optimal hyperplane, it is necessary to minimize the objective functional:

$$\Phi(\mathbf{w}, \xi) = \frac{1}{2}(\mathbf{w} \cdot \mathbf{w}) + C \sum_{i=1}^{l} \xi_i \tag{7}$$

subject to Eq. 6. In functional Φ, addend $C \sum_{i=1}^{l} \xi_i$, where C is user defined parameter, assigns an additional cost for the classification error. Higher value for C leads to a higher error cost.

[1] Neural networks are based on minimization of empirical risk, while keeping the confidence interval constant by selecting a certain construction of learning machine. Consequently, they are subject to overtraining problem.

Wolf's dual problem of minimization of functional Φ is:

$$Max_\alpha L(\alpha) = \sum_i \alpha_i - \frac{1}{2} \sum_{i,j} \alpha_i \alpha_j y_i y_j \mathbf{x_i} \cdot \mathbf{x_j}$$

subject to:

$$\sum_i \alpha_i y_i = 0, 0 \leq \alpha_i \leq C \tag{8}$$

where α_i represent Lagrange multipliers. From Karush–Kuhn–Tucker conditions, only for a number of feature vectors $\mathbf{x_i}$ corresponding Lagrange multipliers α_i differ from zero. These vectors are called support vectors. The solution of Wolf's dual problem 8 is:

$$\mathbf{w} = \sum_{i=1}^{ns} \alpha_i y_i \mathbf{x_i} \tag{9}$$

where ns represents the number of support vectors. Finally, the decision boundary is defined by:

$$f(\mathbf{x}) = sign\left(\sum_{i=1}^{ns} \alpha_i y_i \mathbf{x} \cdot \mathbf{x_i} + b\right) \tag{10}$$

The presented methodology can be applied for nonlinear classifiers by mapping data from the input space into a high-dimensional feature space. It is worth noting that for minimization of functional 8, it is enough to know only the inner product in the high-dimensional feature space. Therefore, it is not necessary to define the high-dimensional feature space in explicit form. Rather opposite, it can be defined using kernel $K(\mathbf{x}, \mathbf{x}_i)$, which represents inner product in the high-dimensional feature space. Introducing $K(\mathbf{x}, \mathbf{x}_i)$, Wolf's dual problem 8 becomes:

$$Max_\alpha L(\alpha) = \sum_i \alpha_i - \frac{1}{2} \sum_{i,j} \alpha_i \alpha_j y_i y_j K(\mathbf{x_i} \cdot \mathbf{x_j})$$

subject to

$$\sum_i \alpha_i y_i = 0, \quad 0 \leq \alpha_i \leq C \tag{11}$$

while the decision boundary is defined by:

$$f(\mathbf{x}) = sign\left(\sum_{i=1}^{ns} \alpha_i y_i K(\mathbf{x}, \mathbf{x_i}) + b\right) \tag{12}$$

and it is a hyperplane in the high-dimensional feature space.

The kernel can be any function that satisfies conditions of Mercer's theorem [46]. For example, these are polynomial kernels (SVM are equivalent to polynomial learning machines in this case), Gauss kernel (SVM are equivalent to radial basis functions machines), sigmoid kernel (SVM are equivalent to two-layer neural networks), and some

wavelets. New kernels can be defined by summing or multiplication of simpler kernels. While deciding on the kernel function, it is necessary to exploit certain a priori knowledge about the problem at hand. After the kernel is chosen, there is only one additional parameter to chose—error cost C.

4 Cylindrical peg-in-hole example

We have elaborated and experimentally verified the contact states recognition machine proposed in Section 3 using a cylindrical peg-in-hole as a standard scenario to validate the force guided assembly. Moreover, the most of industrial assemblies are of this kind. Although this case study may seem simple, it belongs to the class of convex and concave parts mating, and thus, it has at least one contact state made of more than one principle contact.

4.1 Mating force analytical model

Starting from the topological model, a total of six contact states can be distinguished in cylindrical peg-in-hole with chamfer crossing part mating: CS0—no contact, CSc—contact at chamfer; CS1+—one point contact between peg cylinder and boundary edge between chamfer and hole cylinder, CS1−—one point contact between hole cylinder and peg rim, CS2—two point contact, and CSL—line contact (Table 1).

The most interesting contact state among these states is CS2. It has two principal contacts: one point contact between peg cylinder and boundary edge between chamfer and the hole cylinder and one point contact between the hole cylinder and the peg rim. If this CS occurs during the part mating, jamming or wedging can appear, leading to the blocking of the process. Consequently, correct recognition of CS2 is crucial. Besides, it is important to emphasize that, although CS1+ and CS1− look similar, they are essentially different from the aspect of rotating motion that would transfer this contact state into CS0 or CSL.

A quasi-static model can be derived starting from the geometrical model shown in Table 1. It gives dependence of mating forces from the insertion depth for each contact state. Since the main characteristic of mating parts is central symmetry, the whole model is given in the lateral cross section in which the contact has been made. Relations

Table 1 Quasi-static insertion force model for cylindrical peg-into-hole with chamfer crossing: CC—compliance center, i.e., fictive mechanically isotropic peg support with lateral stiffness k_x and angular stiffness k_θ; a and α—chamfer parameters, μ—static Coulomb friction coefficient; e_0 and θ_0—initial position and orientation errors; l—distance from CC to peg's tip; x and θ—position and orientation errors, z—insertion depth; and X_v, Z_v, M_v—generalized insertion force vector components at peg's tip

Geometric representation	CS	X_V, Z_V, M_V
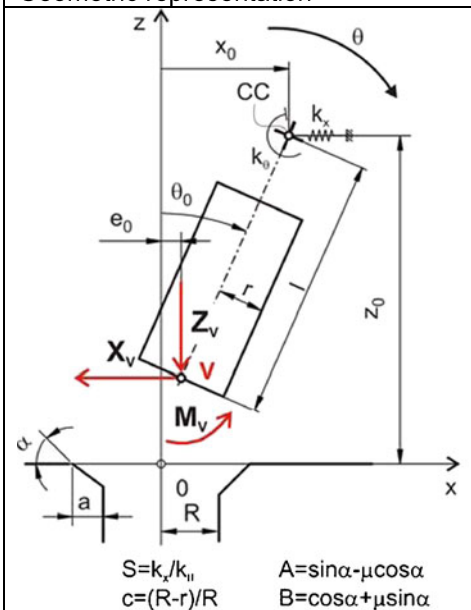	 CSc	$X_V = k_x\left((z'-z)/\operatorname{tg}\alpha\right)/\left(1+Sl\left(l-B/Ar\right)\right)$ $Z_V = k_x B/A\left((z'-z)/\operatorname{tg}\alpha\right)/\left(1+Sl\left(l-B/Ar\right)\right)$ $M_V = k_x B/Ar\left((z'-z)/tg\alpha\right)/\left(1+Sl\left(l-B/Ar\right)\right)$
	 CS1+	$X_V = k_x \dfrac{e_0 - cR - (z+b-l)\theta_0}{1+S(z+b)(z+b-\mu r)}$ $Z_V = \mu k_x \dfrac{e_0 - cR - (z+b-l)\theta_0}{1+S(z+b)(z+b-\mu r)}$ $M_V = (l-(z+b)+\mu r)X_V$
	 CS1-	$X_v = k_x(e_0 - cR)/(1+Sl(l-\mu r))$ $Z_V = \mu k_x(e_0 - cR)/(1+Sl(l-\mu r))$ $M_V = X_v \mu r$
	 CS2	$X_v = k_x\left[cR(1-2l/(l-z-b))+e_0+l\theta_0\right]$ $Z_V = 2\mu\dfrac{M_V - X_V\mu r}{l-(z+b)} - \mu X_V$ $M_V = X_V l - k_\theta(2cR/(l-z-b)-\theta_0)$
	 CSL	$X_v = k_x(e_0 + l\theta_0 - cR)$ $Z_V = \mu k_x(e_0 + l\theta_0 - cR)$ $M_V = k_x(e_0 + l\theta_0 - cR)l - k_\theta\theta_0$

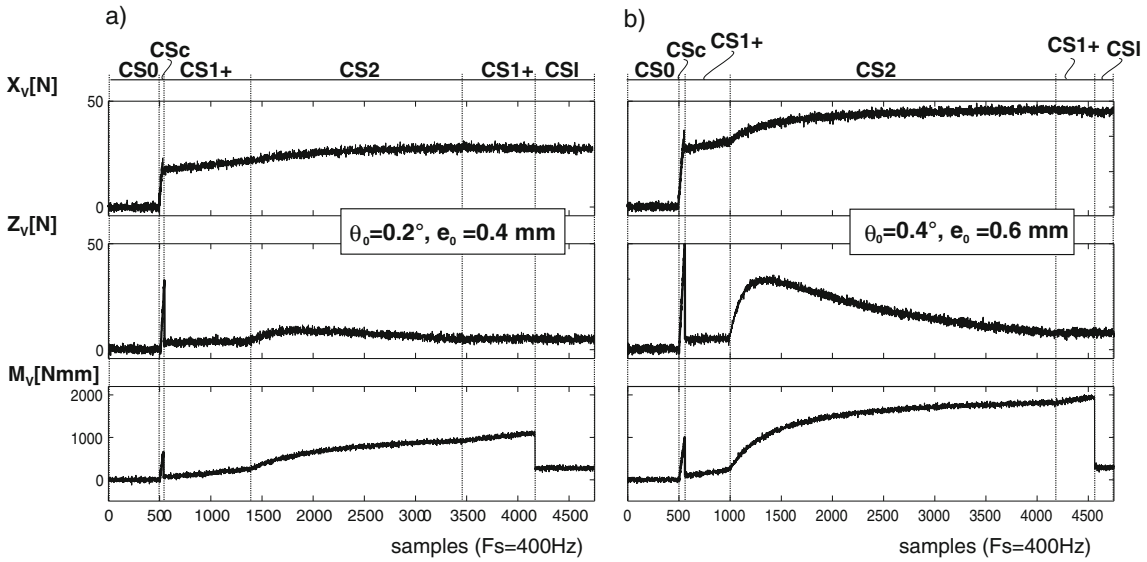

Fig. 5 Insertion force components vs. time for two examples of part mating using developed quasi-static model with added white noise (k_x=60 N/mm, S=0.0005, l=25 mm, R=20 mm, c=0.00105, a=3 mm, α=45°, μ=0.17): **a** e_0=0.4 mm, θ_0=0.2°; **b** e_0=0.6 mm, θ_0=0.4°

describing the dependence of three components of insertion force vector from the insertion depth can be summarized as presented in Table 1. There is a triplet of equations for each contact state. A valid triplet of equations is known only after the contact state has been recognized. The conditions for transition from one contact state to another can be found in [28].

In the given model (Table 1), the following assumptions have been made: (A1) the parts in contact are absolutely rigid, (A2) the friction is Coulomb static friction, (A3) gravitational and inertial forces are neglected, (A4) the position of compliance center does not change with respect to the peg and the hole, (A5) the compliance center has the linear behavior, and (A6) axial stiffness of compliance center is significantly higher than lateral $k_z \gg k_x$. Truly dynamical nature of the part mating process is neglected. Dynamical model of the part mating process which would introduce dynamical nature of friction, elasticity of parts [47], and impact at the contact state transition [48] would be too complex for implementation. Although in the presented model the friction is drastically approximated by a constant, its influence on the generated mating forces according to the given relations is highly significant. Experiments (which will be described in Section 5) have shown that the trends of signals obtained in real world correspond to quasi-static force models. This confirms that the dominant behavior is quasi-static. To make the analytical model closer to reality, the effects of dynamical phenomena (as long as stick-slip is not present) and noise are introduced by adding white noise of 30 dB. The level of noise has been experimentally obtained; the intensity of the noise is considerable, leading to signal-to-noise ratio of 20 dB.

Figure 5 shows time profiles of the insertion force vector, for two examples of part mating using the developed model (quasi-static model with introduced noise). The corresponding contact states are shown in parallel. The only difference between these examples is in the initial position e_0 and orientation θ_0 errors (Fig. 5).

From Table 1 and Fig. 5, it can be concluded that the force components intensities are highly dependent on the initial position e_0 and orientation θ_0 errors which are the inputs for the given model. Values of these errors are unknown, as they come as a result of significant uncertainties that are present in the robotic part mating system.

As can be observed from Fig. 5, the insertion force can have the same intensity level for different contact states

Table 2 Dependence of features X_2 and X_3 from insertion depth for each CS derived from the model (Table 1)

	CSc	CS1+	CS1−	CS2	CSL
X_2	$\frac{B}{A}$	$\frac{1}{\mu}$	$\frac{1}{\mu}$	Nonlinear	$\frac{1}{\mu}$
X_3	r	$\frac{l-(z+b)+\mu r}{\mu}$	r	Nonlinear	Constant

Table 3 The relation between features X_1–X_3 and time derived from Table 2 and Eq. 13

	CSc	CS1+	CS2	CS1−	CSL
X_1	Linear	Nonlinear	Nonlinear	Constant	Constant
X_2	Constant	Constant	Nonlinear	Constant	Constant
X_3	Constant	Linear	Nonlinear	Constant	Constant

even within the single execution of part mating task. Therefore, the features based on the insertion force intensity (i.e., quantitative features) are not discriminative for contact state recognition.

4.2 Feature extraction and selection

Based on the previous analysis, the set of features selected for contact states recognition should be qualitative, i.e., independent of the insertion force intensity. The question is how to derive the set of qualitative features. Our approach is to use the developed quasi-static part mating model. Analytical relations presented in Table 1 contain a specific correlation between CSs and the type of relation between force components and the insertion depth. The relation type between force components and the insertion depth (i.e., whether the relation is constant, linear, or nonlinear) is a truly qualitative feature itself. Further manipulation over the analytical model allows extraction of explicitly qualitative features which uniquely correlate to CSs.

The aforementioned approach can be illustrated through feature extraction and selection for cylindrical part mating. First, from the analytical model we have that the type of relation for all three force components is the same for a given CS. Therefore, we have selected one component—Z_V as the first feature:

$$X_1 = Z_V \tag{13}$$

By further analysis, two additional features can be extracted:

$$X_2 = X_V / Z_V \tag{14}$$

$$X_3 = M_V / Z_V \tag{15}$$

Relations between these two features and the insertion depth for each contact state are shown in Table 2. However, from a practical point of view, the type of relation between the selected features and time is more important. This can be easily obtained since the insertion velocity in robotic part mating is normally constant. Types of changes over time (i.e., constant, linear, and nonlinear) for the extracted features X_1, X_2, and X_3 and for all possible CS are listed in Table 3.

Table 3 shows that the type of relation between features X_1–X_3 and time has a unique combination for each CS. The only exceptions are states CS1− and CSL. Nevertheless, these states do not have to be differed because the same

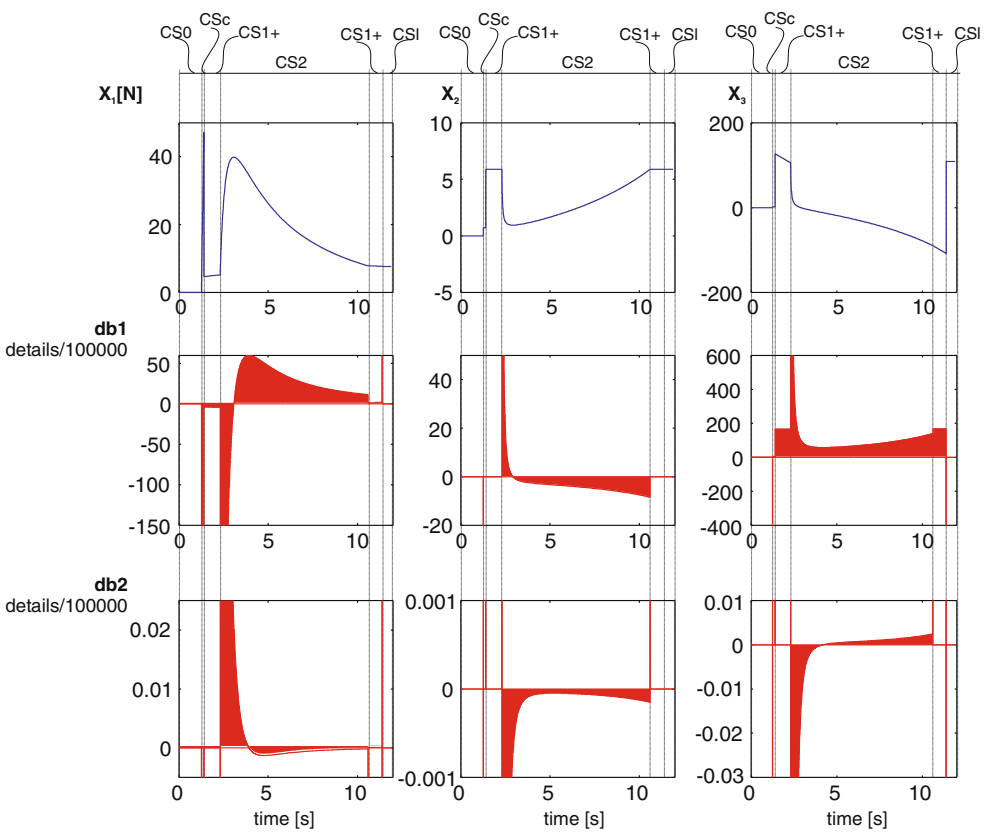

Fig. 6 The force components obtained from quasi-static model along with the first level details coefficients obtained by DWT using db1 and db2; detail coefficients are equal to zero in areas in which the analyzed signal is constant and/or linear, depending on the selected wavelet

Table 4 Detail coefficients for DWT of X_1–X_3 using Haar wavelet: 0—detail coefficients equal to zero and 1—detail coefficients not equal to zero

	CSc	CS1+	CS2	CS1−	CSL
x_1	1	1	1	0	0
x_2	0	0	1	0	0
x_3	0	1	1	0	0

sequence of motion given by the planner can be used in both cases. Moreover, CSL rarely appears in practice.

It is worth noting here that Table 3 has been derived from the analytical model. For practical use, we have to find a way to extract the relation/signal type from nonideal sensory signals. Furthermore, the extraction process has to be performed in real time. Thus, for these purposes, we have used DWT proposed for the CS recognition machine offline training (Fig. 4).

For selection of appropriate wavelet, we exploit the fact that the wavelets from Daubechies family (db wavelets) have the first N vanishing moments [40]:

$$\int x^n \psi(x)\mathrm{d}x = 0, \quad n = 0, 1, \ldots N-1 \tag{16}$$

where N is the order of wavelet ψ. N vanishing moments means that db wavelets of order N are orthogonal to polynomials 1, x, x^2,… x^{N-1} and that the signal DWT is applied so that it will be approximated by polynomials of order $N-1$. In other words, in all regions in which signal is well approximated by a polynomial of order $N-1$, the wavelet coefficients (i.e., detail coefficients) at DWT representation will be equal to zero. To illustrate this property, Fig. 6 shows features X_1–X_3 during one part mating cycle obtained from the quasi-static model along with the detail coefficients of the first level of DWT. We have used the first two wavelets from Daubechies family (db1 and db2). Detail coefficients for db1 (also known as Haar wavelet) are equal to zero in all areas in which signal is constant. For db2 wavelet, detail coefficients are equal to zero in all segments in which the signal is linear or constant.

Summarizing properties defined by relation 16, as well as the relations from Table 3, the fourth level detail coefficients obtained by DWT of X_1, X_2, and X_3 using the db1 wavelet are chosen as representative and discriminative features. Thus, we transform the feature space $\mathbf{X}=[X_1\ X_2\ X_3]$ into a new feature space $\mathbf{x}=[x_1\ x_2\ x_3]$:

$$\mathbf{x} = \mathrm{D}\,W\,\mathrm{T}^4_{db1}(\mathbf{X}) \tag{17}$$

The level of DWT determines the signal history (i.e., number of samples) that will be involved in the current detail coefficient generation (relations 2–4). The fourth level DWT using db1 wavelet requires 16 samples to generate a detail coefficient. Table 4 summarizes the idealized values of features x_1, x_2, and x_3 for all CSs. These features should be equal or close to zero in the areas where the trend of the signal is constant. Thus, they are coded by 0. For all other signal trends, the corresponding features are different from zero, and they are coded by one in Table 4. Practically, this set of extracted features can be considered as a code, which can be used to uniquely code the set of CSs in cylindrical part mating with chamfer crossing.

Before features generation, the signal is de-noised to eliminate not only the noise but also a highly dynamical and stochastic phenomena disregarded in the quasi-static model. Once again, we have utilized DWT for signal de-noising. Conventional de-noising techniques based on IIR or FIR low-pass filters introduce signal distortion. On the other hand, DWT-based de-noising techniques are characterized by phase correctness and good time localization. While choosing the wavelet for de-noising, it is important to have in mind that further signal analysis (extraction of features) will be based on db1 wavelet. Consequently, the wavelet used for de-noising has to be a wavelet of the order higher than one from Daubechies family, or a wavelet from another family. In order to keep the computation time required by de-noising as low as possible, we have chosen wavelet db2.

Figure 7 shows the feature vectors $[x_1\ x_2\ x_3]$ generated using the described procedure from the quasi-static analytical model with aggregated noise. A total of 450,000 patterns have been generated for different part mating cycles with initial errors in the range $e_0 \in [0, 3\ \mathrm{mm}]$ and $\theta_0 \in [0, 1°]$. Since we start from the quasi-static model with aggregated noise, the generated features are not equal but close to zero in the areas where the trend of the signal dominantly behaves as constant.

From the described procedure, it follows that transformations $\mathfrak{I}$ used to generate features from the insertion force have three steps: (1) generation of X_1–X_3 using relations 13–15, (2) DWT-based de-noising using db2, and (3) extraction of features x_1–x_3 using db1 DWT. These transformations are handed over to the online contact states recognition machine (as shown in Fig. 3).

Wavelets used in $\mathfrak{I}$ have not been chosen arbitrarily, but in mathematically consequent manner. We have shown that vanishing moments are an enabling property of Daubechies wavelets. This property makes DWT an extremely powerful tool for feature extraction. Another very important issue is the real-time applicability of DWT.

Exploiting the orthogonality of db wavelets and polynomial functions, we have managed to extract a truly qualitative set of features $[x_1\ x_2\ x_3]$ from the force signal.

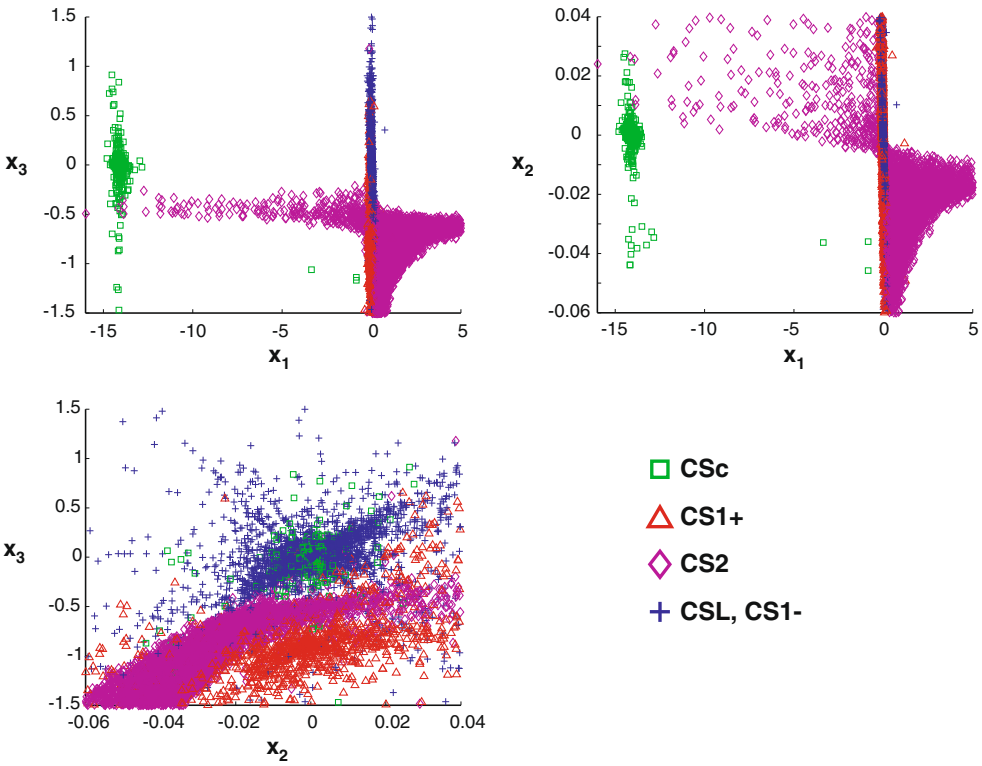

Fig. 7 Representation of the generated patterns in three dimensional feature space; a total of 450,000 patterns for initial error in the range $e_0 \in [0, 3\text{ mm}]$ and $\theta_0 \in [0, 1°]$ are shown along with CSs

These features are independent of the insertion force intensity level, i.e., variation of system's rigidity (k_x, k_θ), friction coefficient (μ), initial pose error (e_0, θ_0) between objects to be mated, chamfer parameters (a, α), etc. They contain the type of relation between force derived features X_1–X_3 and time.

4.3 Feature space partitioning

Following the proposed offline training for CS recognition machine (Fig. 4), we partition the adopted feature space (Eq. 17) using SVM. For simplicity and real-time applicability, we have opted to use a linear kernel function.

Since SVMs are binary classifiers, we propose a hierarchical approach to classify the patterns into multiple classes. At each level of classification, one contact state is separated from the remaining contact states. From Table 4, it follows that the classification can be monothetic, meaning that only two out of three generated features can be used for separating each of the contact states.

At step 0, based on intensity of Z_V, force component CS0 is separated, as a contact state in which the value of this force is $Z_V < Z_{V\text{const}}$ ($Z_V = X_1$). The value of the constant $Z_{V\text{const}} = 5$ N is experimentally identified.

At the first step of the classification, CSc is separated using features x_1 and x_3. It should be emphasized that, although the classes are well separable (thanks to the choice of features), the classification is very unfavorable from the classes' size point of view. CSc contains only 3% of the total number of generated patterns. When such a large difference in class sizes is at hand, classification methods based on probability density estimation (e.g., k nearest neighbors, Parzen probability density estimation) and methods based on minimization of criterion function usually perform poorly. In these cases, the large class becomes dominant and masks the influence of the small. On the other hand, SVM show good classification

Table 5 Classification steps

Classification step i	Separated CS	Features	$\mathbf{w_i}(1)$	$\mathbf{w_i}(2)$	b_i
0	CS0	Value of Z_V	–	–	–
1	CSc	x_1 and x_3	1.14	−0.63	−14.33
2	CS2	x_1 and x_2	−17.55	5.48	−1.61
3	CS1+ and CS1−/CSL	x_2 and x_3	31.88	−12.58	4.97

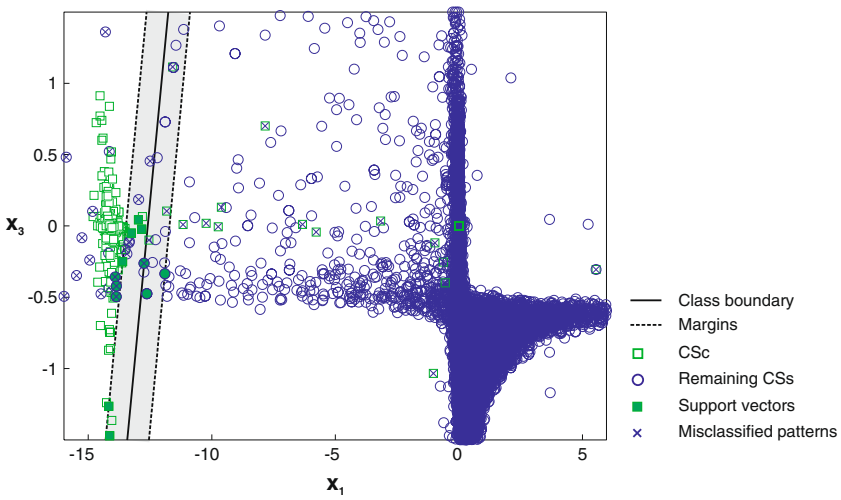

Fig. 8 Class boundary—the optimal hyperplane for the first step of classification; CSc is separated from the remaining CSs

properties regardless the size of classes. When SVM are used for classification, the patterns closer to the class boundaries are more significant than those far away.

For SVM training, parameter C=10 is heuristically chosen. The class boundary is defined using the relation:

$$\mathbf{w_1}(1)x_1 + \mathbf{w_1}(2)x_3 = b_1 \tag{18}$$

The values of $\mathbf{w_1}$ and b_1 are shown in Table 5. Using SVM, we have obtained the margin: Δ_1=0.7689.

Classification results are shown in Fig. 8. The share of support vectors in the total training set is 0.05%. Within the classes, the share of support vectors is 0.70% for CSc and 0.02% for the rest of CSs. The percentage of misclassification over the total training set is 0.06% for CSc and 0.08% for the second class; that is, within classes, the percentage is 1.8% for CSc and 0.09% for the second class.

At the second step of classification, CS2 is separated based on features x_1 and x_2. In the total training set 48.18% patterns belongs to CS2. In this case, parameter C is set to 200, and the class boundary is defined by:

$$\mathbf{w_2}(1)x_1 + \mathbf{w_2}(2)x_2 = b_2 \tag{19}$$

The values of $\mathbf{w_2}$ and b_2 are shown in Table 5. In this classification, the margin is Δ_2=0.0544.

The results of classification are presented in Fig. 9. The share of support vectors in the total training set is 0.77%, while this share within the classes is 0.80% for CS2 and 0.74% for the rest of CSs. The percentage of misclassification over the total training set is 3.28% for CS2 and 1.36% for the second class, that is, within classes 6.81% for CS2 and 2.63% for the second class. Within the margins, there are 2.31% of misclassified patterns for CS2 and 0.55% for the second class. Furthermore, within the classes, this is 4.80% misclassified patterns for CS2 and 1.06% for the remaining contact states.

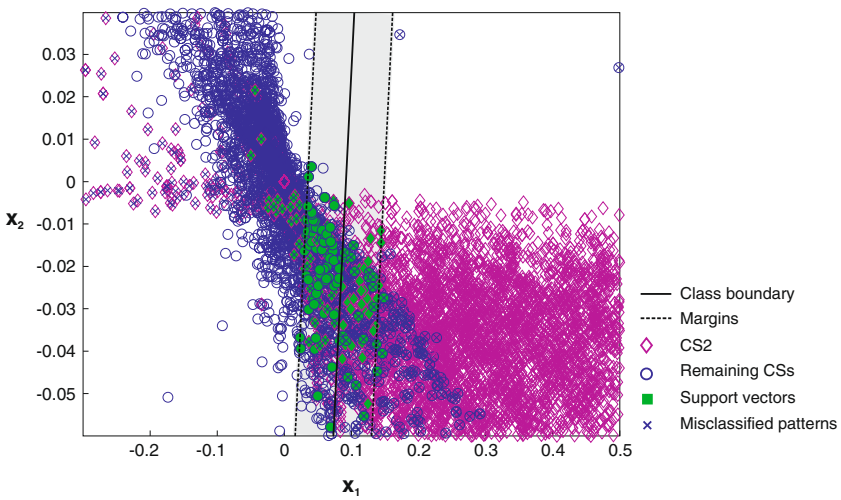

Fig. 9 Class boundary—the optimal hyperplane for the second step of classification; CS2 is separated from the remaining CSs

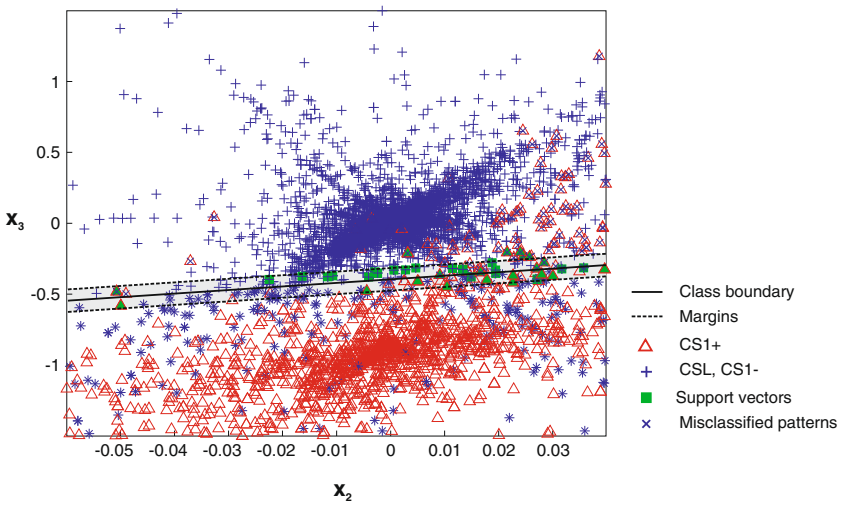

Fig. 10 Class boundary—the optimal hyperplane for the third step of classification; CS1+ and CSL/CS1− are separated

At the third level of classification contact states, CS1+ and CS1−/CSL are separated based on features x_2 and x_3. Here, 16.84% of patterns belong to CS1+. In this case, parameter C has been set to 300, and the class boundary is described by:

$$\mathbf{w_3}(1)x_2 + \mathbf{w_3}(2)x_3 = b_3 \tag{20}$$

The values of $\mathbf{w_3}$ and b_3 are shown in Table 5. For this classification, the obtained margin is Δ_3=0.029.

The results of classification are depicted in Fig. 10. The share of support vectors in the total training set is 3.00%. Within the classes, 5.30% of patterns in the CS1+ and 2.53% in the CS1−/CSL are support vectors. The percentage of misclassification over the total training set is 0.73% for CS1+ and 1.95% for CS1−/CSL. Expressed within the classes, 4.34% of patterns in CS1+ and 2.34% of patterns in the second class are misclassified. Within the margins, there is 0.62% misclassified patterns in the class CS1+ and 1.50% in the class CS1−/CSL. Given within the classes, inside the margins are 3.66% of misclassified patterns for the class CS1+ and 1.80% for the class CS1−/CSL.

Identified class boundaries (Eqs. 18–20) represent the optimal separating hyperplanes. Using these hyperplanes, the feature space is optimally partitioned. This partition is handed over to the online CS recognition machine. Note that the inherent maximal margins lead to robust online classification performance.

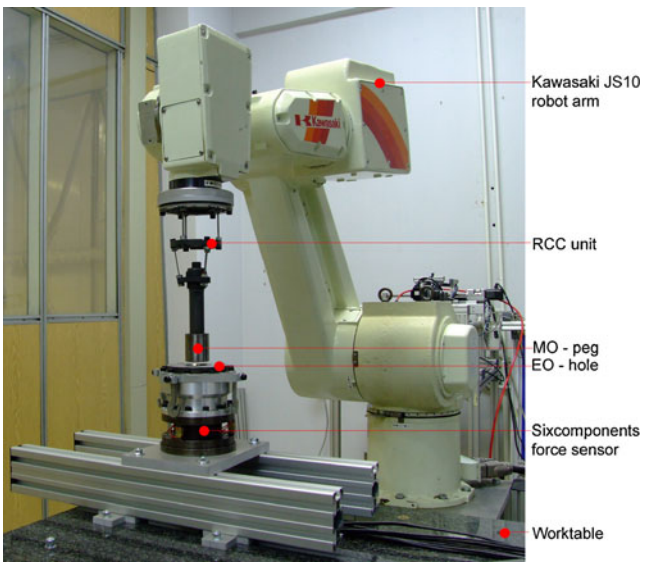

Fig. 11 Experimental installation

5 Experimental verification

The proposed CS recognition machine is experimentally verified using laboratory installation shown in Fig. 11. It is based on Kawasaki JS10 6DOF robot arm with a custom-made Remote Center Compliance unit placed at the robot tip. The payload of robot is 10 kg. For the force measurements, we have used a six-component, software-decoupled, custom-made strain-gauge force sensor. The sensor is put on the worktable, and EO with a hole is placed on it. The mating parts have nominal diameter D=40 mm and the clearance of 20 μm. This gives the clearance ratio $c=(D-d)/D=5\times10^{-4}$. The chamfer is 3/45°, and the mating parts are made of cemented steel, HRC 60, surfaces grinded to IT5.

A large number of experiments were carried out. Figure 12b shows Z_V component obtained during one typical part mating cycle along with the results of recognition of CSs using the proposed machine.

Figure 12a shows force components X_V, Z_V, and M_V that have been measured during this experiment. Force signal is

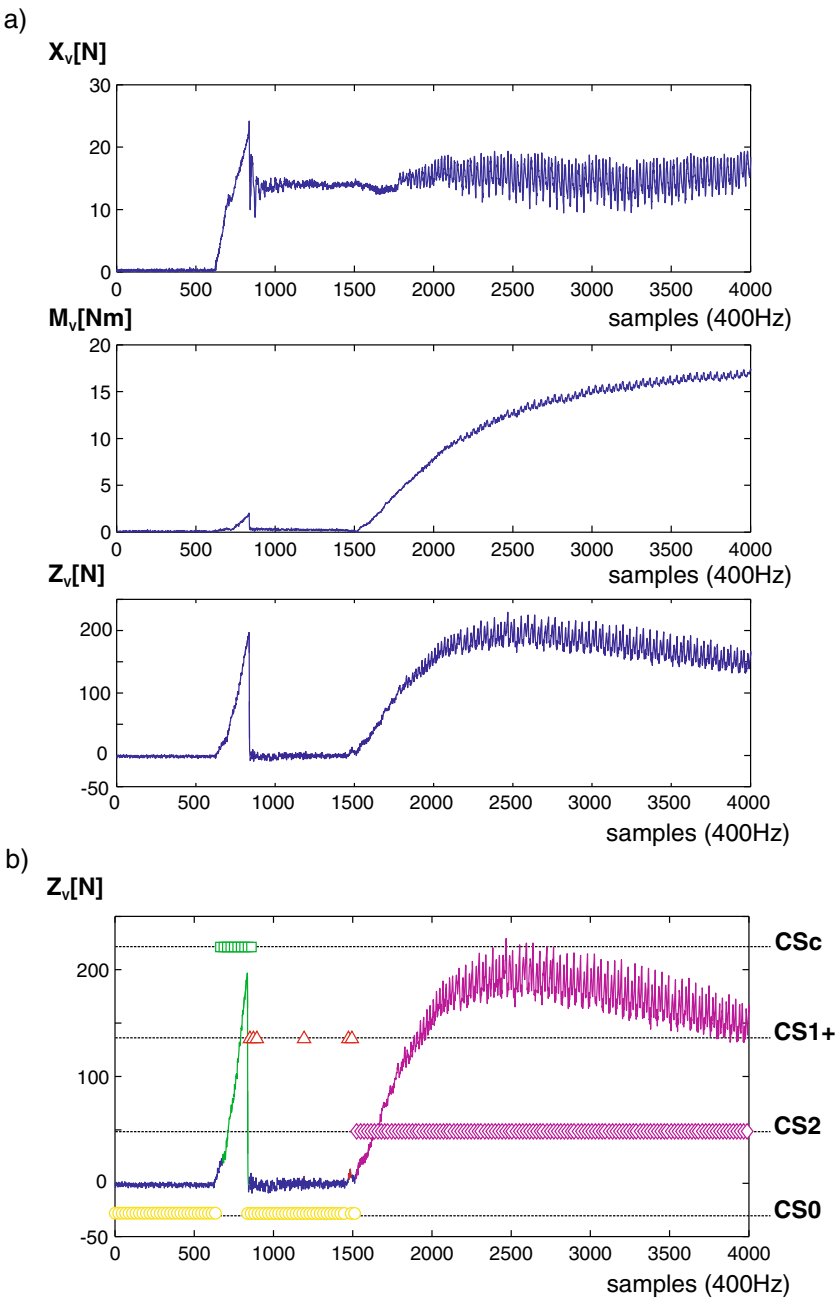

Fig. 12 **a** Force components X_V, M_V, and Z_V obtained experimentally during one typical part mating cycle; **b** force component Z_V along with the results of CS recognition during the same part mating cycle

sampled by 400 Hz. For features generation, we have used the fourth level db1 DWT that requires a buffer of 16 samples. In this setup, the time required for the CS recognition is 40 ms.

Since the exact position and orientation of the peg's tip as well as a relative position of EO to the robot were unknown, it was not possible to know in each instant in which contact state were the parts during the experiment. Consequently, we have not been able to extract efficiency of the recognition machine in percentage of correctly identified CSs. Nevertheless, it is evident that an excellent correlation of the part mating CS sequence, force signals, and the recognized CSs has been achieved. Since the training (i.e., synthesis of the recognition machine) has been carried out based on the analytical model, achieved efficiency of CSs recognition from real-world sensory data is unexpectedly well.

6 Conclusion

In this paper, we have proposed a new framework for generation of a contact states recognition machine that can

be used in robotic part mating. Although the contact states are primarily determined by geometry and relative positions of the objects to be assembled, we have shown that due to the dynamical nature of the part mating, they can be recognized based on the generalized mating force.

We have proposed a model-based CS recognition machine. This is a novel approach, which introduces significant advantages over commonly used methods that are strictly based on experimental data. While designing the recognition machine, we have systematically exploited the a priori knowledge contained in the analytical model of the part mating process

The analytical model provides information about CS that corresponds to the generated force vector. This information enables the supervised training. We have utilized SVM for partition of the adopted feature space. It is worth noting that when experimentally obtained data are exclusively used in the training procedure, it is not possible to utilize SVM which demand supervised training. In our case (i.e., when an analytical model is used), the excellent generalization properties of SVM could be exploited. However, SVM have a limitation that they are binary classifiers. To overcome this, we have proposed a hierarchical approach where at each classification level one class is separated from the remaining classes. This approach enables classification into multiple classes.

Furthermore, the analytical model enables extraction of truly qualitative features. We use these features to create a generally applicable machine insensitive to process parameters variations. We propose utilization of DWT for feature extraction.

Utilization of the training procedure based on a mechanical model made numerous experiments unnecessary. These experiments might have questionable outcomes due to the significant uncertainties and small clearances in the part mating process.

The proposed approach is elaborated and experimentally verified using an example of cylindrical peg-in-hole with chamfer crossing part mating. Instead of choosing the wavelet for features extraction intuitively, arbitrarily or by trial and error (which is a common practice), we have shown how analytical properties of certain wavelets can be used for effective extraction of qualitative features. In this example, features and class boundaries are formally obtained without the black box approach. This would not be possible if the training was based on experimental data.

The machine created using our approach can be generally applied for cylindrical part mating with chamfer crossing. Although the training was based on approximate, i.e., significantly simplified analytical model, experiments have shown that the overall performance of CS recognition machine in real world was excellent.

Acknowledgments We wish to express our gratitude to the Ministry of Education and Science of Serbia for providing financial support under the grant TR35007.

References

1. Scholz-Reiter B, Freitag M (2007) Autonomous processes in assembly systems. CIRP Ann 56:712–729
2. Chen H, Fuhlbrigge TA, Zhang G (2007) Towards intelligent robotic assembly: trends in industry. Assembly Automation 27: Viewpont
3. Chen CW (2011) Stability analysis and robustness design of nonlinear systems: an NN-based approach. Appl Soft Comput 11:2735–2742
4. Chen CW (2011) Modeling and control for nonlinear structural systems via a NN-based approach. Expert Syst Appl 38:7837–7850
5. Hsiao FH, Chen CW, Liang YW, Xu SD, Chiang WL (2005) T-S fuzzy controllers for nonlinear interconnected systems with multiple time delays. IEEE Trans Circuits and Syst—I: Regul Pap 52:1883–1893
6. Bouakrif F (2010) Reference model iterative learning control for nonlinear systems with repeatable and non-repeatable uncertainties. Int J Adv Manuf Technol 51:1159–1169
7. Lin J, Lian RJ (2011) Hybrid self-organizing fuzzy and radial basis-function neural-network controller for constant cutting force in turning. Int J Adv Manuf Technol 53:921–933
8. Desai RS, Volz R (1989) Identification and verification of termination conditions in fine motions in presence of sensor errors and geometric uncertainties. In: Proceedings of IEEE international conference on robotics and automation, pp 800–806
9. Hirukawa H, Matsui T, Takase K (1994) Automatic determination of possible velocity and applicable force of frictionless objects in contact from a geometric model. IEEE Trans on Rob Autom 10:309–322
10. Mosemann H, Raue A, Wahl F (1999) Identification of assembly process states using polyhedral convex cones. In: Proceedings of IEEE international conference on robotics and automation, Detroit, MI, USA, pp 2756–2761
11. Xiao J, Liu L (1998) Contact states, representation and recognizability in the presence of uncertainties. In: Proceedings of international conference on intelligent robots and systems, Victoria, Canada, pp 1151–1156
12. Xiao J, Zhang L (1996) Towards obtaining all possible contacts—growing a polyhedron by its location uncertainty. IEEE Trans on Rob and Autom 12:553–565
13. Farahat AO, Graves BS, Trinkle JC (1995) Identifying contact formations in the presence of uncertainty. In: Proceedings of international conference on intelligent robots and systems, Pittsburg, PA, USA, Volume 3, pp 59–64
14. Suárez R, Basañez L, Rosell J (1994) Assembly contact force domains in the presence of uncertainty. In: Proceedings of fourth IFAC symposium on robot control, Capri, Italy, pp 653–659
15. De Schutter J, Bruyninckx H, Dutré S, De Geeter J, Katupitiya J, Demeery S, Lefebvre T (1999) Estimating first-order geometric parameters and monitoring contact transitions during force-controlled compliant motions. Int J Rob Res 18:1161–1184
16. Lefebvre T, Bruyninckx H, De Schutter J (2003) Polyhedral contact formation modeling and identification for autonomous compliant motion. IEEE Trans Rob 19:26–41
17. Lefebvre T, Bruyninckx H, De Schutter J (2005) Polyhedral contact formation identification for autonomous compliant motion: exact nonlinear Bayesian filtering. IEEE Trans Rob 21:124–129

18. Lefebvre T, Bruyninckx H, De Schutter J (2005) Online statistical model recognition and state estimation for autonomous compliant motion, systems. IEEE Trans Syst, Man Cybern C Appl Rev 35:16–29
19. Gadeyne K, Lefebvre T, Bruyninckx H (2005) Bayesian hybrid model-state estimation applied to simultaneous contact formation recognition and geometrical parameter estimation. Int J Rob Res 24:615–630
20. Nuttin M, Rosell J, Suárez R, Van Brussel H, Basañez L, Hao J (1995) Learning approaches to contact estimation in assembly tasks with robots. In: Proceedings of the 3rd European workshop on learning robots, Heraklion, pp 1–11
21. Skubic M, Volz RA (2000) Identifying single-ended contact formations from force sensor patterns. IEEE Trans Rob Autom 16:597–603
22. Everett LJ, Ravari R, Volz RA, Skubic M (1999) Generalized recognition of single-ended contact formations. IEEE Trans Rob Autom 15:829–836
23. Cervera E, del Pobil AP (2002) Sensor-based learning for practical planning of fine motions in robotics. Int J Inf Sci 145:147–169
24. Brignone LM, Howarth M (2002) A geometrically validated approach to autonomous robotic assembly. In: Proceedings of international conference on intelligent robots and systems, Lausanne, pp 1626–1631
25. Park YK, Cho HS (1994) A self-learning rule-based control algorithm for chamferless part mating. Control Eng Pract 2:773–783
26. Son C (2001) A neural/fuzzy optimal process model for robotic part assembly. Int J Mach Tool Manuf 41:1783–1794
27. Son C (2002) Optimal control planning strategies with fuzzy entropy for robotic part assembly tasks. Int J Mach Tool Manuf 42:1335–1344
28. Whitney DE (1982) Quasi-static assembly of compliantly supported rigid parts. Trans ASME, J Dyn Syst Meas Control 104:65–77
29. Hannaford B, Lee P (1991) Hidden Markov model analysis of force/torque information in telemanipulation. Int J Rob Res 10:528–539
30. Hovland GE, McCarragher BJ (1998) Hidden Markov models as a process monitor in robotic assembly. Int J Rob Res 17:153–168
31. Lau HYK (2003) A hidden Markov model-based assembly contact recognition system. Mechatronics 13:1001–1023
32. Debus T, Dupont P, Howe R (2004) Contact state estimation using multiple model estimation and hidden Markov models. Int J Rob Res 23:399–413
33. McCarragher BJ, Asada H (1993) Qualitative template matching using dynamic process models for state transition recognition of robotic assembly. Trans ASME J Dyn Syst Meas Control 115:261–269
34. Sikka P, McCarragher B J (1997) Rule-based contact monitoring using examples obtained by task demonstration. In: Proceedings of the 15th international joint conference on artificial intelligence, Nagoya, Japan, pp 514–521
35. Shirinzadeh B, Zhong Y, Tilakaratna PDW, Tian Y, Dalvand MM (2011) A hybrid contact state analysis methodology for robotic-based adjustment of cylindrical pair. Int J Adv Manuf Technol 52:329–342
36. Dietrich F, Buchholz D, Wobbe F, Sowinski F, Raatz A, Schumacher W, Wahl FM (2010) On contact models for assembly tasks: experimental investigation beyond the peg-in-hole problem on the example of force-torque maps. In: Proceedings of the 2010 IEEE/RSJ international conference on intelligent robots and systems, Taipei, Taiwan, pp 2313–2318
37. Jakovljevic Z, Petrovic PB (2010) Recognition of contact states in robotized assembly using qualitative wavelet based features and support vector machines. In: Hinduja S, Li L (eds) Proceedings of the 36th international MATADOR conference, 1st edn. Springer, London, pp 305–308
38. Lefebvre T, Xiao J, Bruyninckx H, De Gersem G (2005) Active compliant motion: a survey. Adv Rob 19:479–499
39. Petrovic PB (2003) Outline of a new feature space deformation approach in fuzzy pattern recognition. FME Trans 31:75–86
40. Daubechies I (1992) Ten lectures on wavelets. In: CBMS-NSF regional conference series in applied mathematics, 61. SIAM, Philadelphia
41. Mallat SG (1989) A theory for multiresolution signal decomposition: the wavelet representation. IEEE Trans Pattern Anal and Mach Intell II:674–693
42. Teti R, Jemielniak K, Dornfeld D (2010) Advanced monitoring of machining operations. CIRP Ann Manuf Technol 59:717–739
43. Liu H, Chen Y, Peng X, Xie J (2011) A classification method of glass defect based on multiresolution and information fusion. Int J Adv Manuf Technol. doi:10.1007/s00170-011-3248-z
44. Sevilla-Camacho PY, Herrera-Ruiz G, Robles-Ocampo JB, Jáuregui-Correa JC (2011) Tool breakage detection in CNC high-speed milling based in feed-motor current signals. Int J Adv Manuf Technol 53:1141–1148
45. Petrovic PB, Jakovljevic Z, Milacic VR (2010) Context sensitive recognition of abrupt changes in cutting process. Expert Syst Appl 37:3721–3729
46. Vapnik VN (2000) The nature of statistical learning theory. Springer, New York
47. Xia Y, Yin Y, Chen Z (2006) Dynamic analysis for peg-in-hole assembly with contact deformation. Int J Adv Manuf Technol 30:118–128
48. Vukobratovic M, Potkonjak V, Matijevic V (2001) Contribution to the study of dynamics and dynamic control of robots interacting with dynamic environment. Robotica 19:149–161